A&A manuscript no.
(will be inserted by hand later)

Your thesaurus codes are:
07(08.01.3; 08.05.1; 08.06.3; 08.19.3; 08.23.3; 10.15.2)

ASTRONOMY AND ASTROPHYSICS

September 5, 2000

An analysis of HST UV spectra of Cyg OB2 stars⋆

A. Herrero[1,2], J. Puls[3], L.J. Corral[1] and R.P. Kudritzki[3,4]

[1] Instituto de Astrofísica de Canarias, E-38200 La Laguna, Tenerife, Spain
[2] Departamento de Astrofísica, Universidad de La Laguna, Avda. Astrofísico Francisco Sánchez, s/n, E-38071 La Laguna, Spain
[3] Universitäts-Sternwarte München, Scheinerstr. 1, D-81679 München, Germany
[4] Institute for Astronomy, University of Hawaii, 2680 Woodlawn Drive, Honolulu, Hawaii 96822, USA

received date; accepted date

Abstract. As a first step of a vigorous program to investigate the Wind Momentum – Luminosity Relationship (WLR) of Galactic O-stars by analyzing stars belonging to the same cluster we present UV HST observations of six supergiants and one giant in the Cyg OB2 association. Terminal and turbulent wind velocities, velocity laws and metal ion column densities are derived and mean ionization fractions are estimated. Turbulent velocities are mostly in the range 10 – 14 % of v_∞. The terminal velocities agree well with the average v_∞ vs. spectral class relationship compiled by Kudritzki and Puls (2000). We compare the observed v_∞ vs. escape velocity (depending on the diagnostics of the stellar mass) correlation with the predictions of the radiatively driven wind theory and find better agreement with the spectroscopic masses rather than with the evolutionary ones. The β velocity field exponents are in the range 0.7 – 0.8, without any trend towards larger values.

We show that for a single luminosity class there is a tight relationship between $T_{\rm eff}$ and $< \rho >$ (the mean density at the point in the stellar wind, where half the wind terminal velocity is reached). In consequence, the ionization fractions show the same trend with both, $T_{\rm eff}$ and $< \rho >$: we find that N V increases with $T_{\rm eff}$, Si IV decreases and C IV does not clearly correlate.

As a byproduct, we also derive interestellar H I column densities towards Cyg OB2, which turn out to be quite large. For one object (Cyg OB2#2) we find inconsistencies making the association membership questionable.

Key words: stars: atmospheres – stars: early-types – stars: supergiants – stars: fundamental parameters – stars: winds, outflows – Galaxy: open clusters and associations: individual: Cyg OB2

1. Introduction

One of the most promising achievments with respect to the physics of radiatively driven winds from massive stars is the notion that a simple analysis of their spectra enables the derivation of their distances, on basis of the so-called Wind Momentum – Luminosity Relation (WLR), provided that this relation has been accurately calibrated for metallicity and spectral class. Given these conditions it has been shown (McCarthy et al., 1997, Kudritzki et al., 1999) that the WLR can be used to derive extragalactic distances within 20 Mpc, reaching the Virgo and Fornax clusters. As the metallicity of the target stars will not be known in advance, one has to calibrate the WLR for an appropriate range as large as possible. To this end, a number of programs have been started using objects with known distances in the Milky Way, the Magellanic Clouds, M31 and M33.

The major problem for the calibration of the Galactic WLR arises from the scatter introduced by uncertainties in distance. Even the latest data compiled by Kudritzki & Puls (2000) do still not reach an accuracy that would allow a realistic *application* of the method: although the data that have been used are based on stars belonging to open clusters, the relative errors between their distances are sufficient to introduce a significant scatter into the derived WLR. In order to improve this situation (in a first step for O-type supergiants), we have decided to observe a number of stars belonging to the *same* cluster and analyze them in a completely consistent way.

We have chosen the Cyg OB2 association for several reasons: (a) it contains a large number of O stars; (b) it has been studied, photometrically and spectroscopically, by Massey & Thompson (1991), who provide magnitudes and reddenings and derive a distance modulus of 11.2 ± 0.2; and (c) we have already accumulated optical observations and performed a plane-parallel analysis, which is a prerequisite for deriving mass-loss rates by means of spherical models (Herrero et al., 1999, 2000).

In addition, Cyg OB2 is very interesting by its own. It contains the largest known concentration of OB stars in the Galaxy and their properties resemble those in young globular clusters in the LMC (Knödlseder, 2000). Cyg OB2 contains several stars with initial masses of the order of 100 $M_\odot$ (Herrero et al., 1999, 2000; Massey & Thompson, 1991; Knödlseder, 2000) and one of the few known O3 stars (Cyg OB2#7) as well as one of the most luminous objects in the Milky Way (VI Cyg, or Cyg OB2#12) (see Massey & Thompson, 1991, and references therein). Thus, all information that we can gather about

Send offprint requests to: A. Herrero
⋆ Partly based on INES data from the IUE satellite
Correspondence to: ahd@ll.iac.es

this association and its members will be of more general importance.

In this paper we present and analyze HST UV spectra originally obtained with the major goal of deriving terminal velocities. Note that the terminal velocities for Cyg OB2 stars provided by Leitherer et al. (1982) were only estimated from Copernicus observations of stars with similar spectral types, except for one object, Cyg OB2#8A, which had been observed by IUE. In a follow-up paper then, we will perform a consistent analysis of the optical spectra by means of spherical models and using the values for terminal velocities derived here, in order to obtain mass-loss rates and to provide the desired additional points for the calibration of the Galactic WLR.

This paper is organized as follows. Sect. 2 presents the characteristics of the observations, and the spectra are described in Sect. 3. In Sect. 4 we analyze the interstellar extinction, and the available UV resonance lines are investigated in Sect. 5, with some individual comments given in Sect. 6. In addition to determining terminal velocities, we derive also mean ionization fractions, using here the presently available Galactic WLR in a preliminary way. (By means of the detailed mass-loss rates expected from our follow-up paper, these numbers can be easily improved). The results obtained by our analysis are discussed in Sect. 7, and we finish with conclusions and future aspects in Sect. 8.

2. The observations

Observations were made with the HST STIS, using the GL140 grating which provides a resolution from 310 to 210 km s^{-1} in the wavelength range from 1150 to 1700 Å. We used a $0.''2$ wide slit, which is recommended for optimizing the spectral purity. Table 1 gives our list of objects and other details of the observations.

After having received the spectra we first rectified the continuum by tracing a polynom through a number of selected continuum points chosen iteratively. Several factors had to be taken into account during this process: (a) the blue part of the spectrum is uncertain due to lack of flux or sensitivity; (b) the N V $\lambda\lambda$1237–42 doublet is contaminated by interstellar L_α absorption. A fit to L_α has been performed to derive hydrogen column densities (see Sect. 4) and to correct for the contamination, but due to the strength of L_α towards Cyg OB2 this correction affects strongly the continuum definition close to N V; in this range then, the rectification had to be done iteratively; (c) early type objects (O3 – O5) show considerable line–blocking from Fe V between Si IV and C IV, while (d) later types show very strong line blocking redwards of C IV(including this line), also mainly due to iron. The effect increases towards later spectral types.

The definition of the continuum can be slightly inaccurate in these ranges, and only a self–consistent calculation can give better results. However, these uncertainties do not seriously affect the analysis of the resonance lines under question, in particular not the derivation of terminal velocities.

A second point that had to be taken into account concerns the wavelength calibration. The STIS Instrument Handbook indicates that the absolute calibration is accurate up to 1 pixel and that the relative calibration is typically .25 pixel, corresponding to about 50 km s^{-1}. For two of our objects we have found discrepancies in the wavelength calibration that correspond to this accuracy, by comparing to positions of IS lines. We have corrected the relative discrepancy by refering all scales to that of Cyg OB2 #7, which has a radial velocity (as derived from optical spectra) of only 10 km/s, and where the IS lines lie at their theoretical positions. For the two objects mentioned above, Cyg OB2 #8A and Cyg OB2 #4, a final correction to the blue (by 94 and 46 km s^{-1}, respectively) turned out to be necessary.

3. Description of the spectra

After all the above corrections have been performed, we finally obtained the spectra displayed in Fig. 1.

The UV spectral morphology of the observed Cyg OB2 stars appears to be “normal”, in agreement with previous works on Galactic OB stars. However, one interesting contribution of the present work is the presentation of spectra of three O5 supergiants, a spectral class which is underrepresented in the IUE archive (where HD 14 947 is the only Galactic object with that classification.) In the following we briefly comment on several morphological aspects of our spectra.

3.1. N V

Fig. 2 displays the N V region of the spectrum in more detail, indicating the actual degree of saturation of this line after correction for L_α absorption. N V is heavily saturated in the O3 object, while all O5 stars show a non-saturated profile. This is in agreement with the spectrum of HD 14 947 displayed by Walborn et al. (1985), although it does not agree with the newly reduced spectrum contained in the Final IUE Archive. The line weakens towards later spectral types and is no longer visible at B1.

3.2. Si IV

Together with C IV, for most of our objects we used this doublet as primary indicator for terminal velocities. It is very weak at O3, photospheric at B1 and shows a strong luminosity effect in the intermediate types, being weaker in the O7 giant (cyg OB2#4). The profile does not saturate in any object.

3.3. C IV

The line is close to saturation in all objects earlier than O9, and reaches the error flux level in Cyg OB2#7 and #8C. The coolest object, Cyg OB2#2, shows a nearly symmetric, pure absorption profile. We note here that a certain variability in the blue edge is indicated when comparing the two spectra taken for Cyg OB2 #11. We will later see that this affects slightly the value of the derived turbulent velocity. We also note that

Table 1. Cyg OB2 stars observed with HST/STIS. All numerical identifications are taken from Schulte (1958). Magnitudes and positions for epoch 1950.0 have been taken from Massey & Thomson (1991) and precessed within IRAF for epoch 2000.0. Spectral types are also from Massey & Thompson, except for Cyg OB2 #11 and #4, that are taken from Walborn (1973). The observing dates were October, 19th (1) and 20th (2) 1999. An asterisk besides the exposure time indicates that two spectra were acquired and added. S/N ratios are given per pixel and have been estimated using the STIS software.

Ident	α(2000)	δ(2000)	V mag.	Spectral Type	Obs. Date	Exp. time(s)	S/N
7	20:33:14.1	41:20:22.0	10.55	O3 If	2	5521*	19
11	20:34:08.6	41:36:59.6	10.03	O5 If$^+$	1	5521*	36
8C	20:33:18.0	41:15:31.1	10.19	O5 If	1	2497	19
8A	20:33:15.1	41:18:50.5	9.06	O5.5 I(f)	1	2452	34
4	20:32:13.8	41:27:13.9	10.23	O7 III((f))	2	2497	27
10	20:33:46.1	41:33:01.4	9.88	O9.5 I	1	5521*	25
2	20:31:22.0	41:31:28.2	10.64	B1 I	1,2	5397*	38

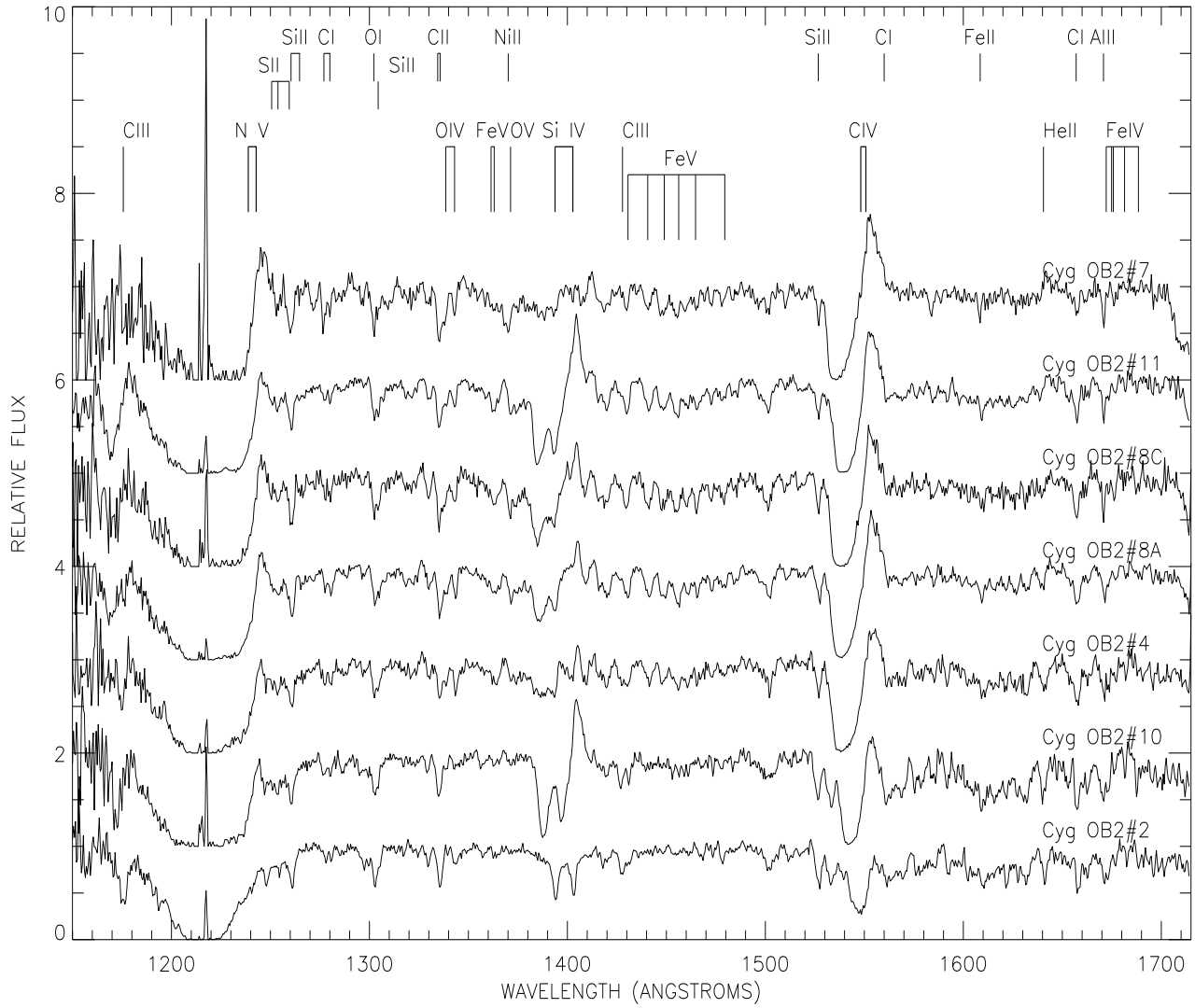

Fig. 1. The observed rectified UV spectra. Relative fluxes have been arbitrarily displaced in ordinates for the sake of clarity. The main IS lines are marked at the top, and below we have indicated the rest wavelengths of the most important stellar lines.

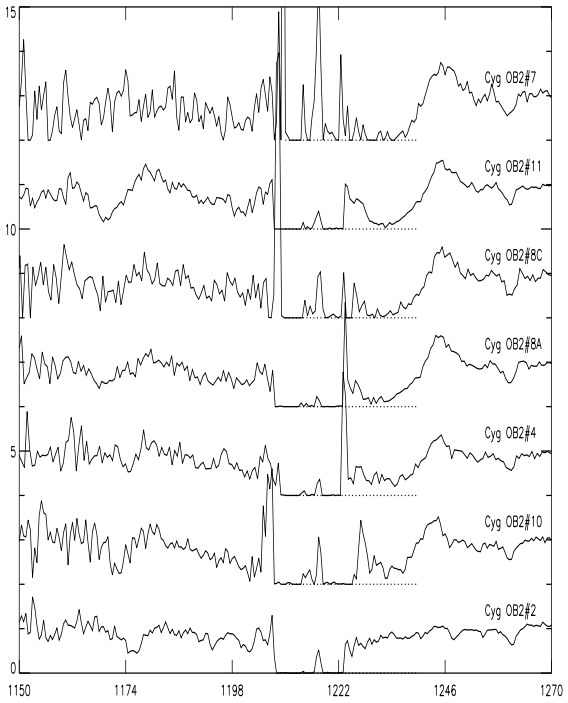

Fig. 2. The observed N V spectra corrected for Ly$_\alpha$ absorption. Spectra have been arbitrarily displaced in ordinates, and horizontal lines have been drawn at individual zero flux level to indicate the degree of saturation. In all O5 supergiants, the doublet is close to saturation, but without actually reaching zero level. (Wavelengths in Å.)

Cyg OB2#10 (O9.5 I) displays a P-Cygni type profile on top of a heavily blocked pseudocontinuum (which complicates the continuum rectification in this region, see above).

3.4. Other features

The UV spectra of early supergiants are line rich, although their interpretation is somehow complicated by the IS lines. We have marked the most important IS as well as stellar lines on top of Fig. 1. The wide range in spectral types helps to distinguish between both classes when the lines lie close to each other. The positions of a number of Fe V and Fe IV lines which dominate the stellar spectra in the regions 1350 – 1550 Å and 1600 – 1700 Å, respectively, are indicated, and in particular in earlier spectral types Fe V can be unambigously identified. The development of C III λ1428 towards later spectral types and of O V λ1371 towards earlier types is also clearly seen. Finally, we like to point at the behaviour of He II λ1640, going from emission in O3 to absorption in later types.

4. Interstellar extinction

We have derived H I column densities towards Cyg OB2 by fitting the IS L$_\alpha$ line, which is also important for the correction of the N V $\lambda\lambda$1237, 1242 doublet, as pointed out above. Note that, vice versa, the red wing of L$_\alpha$ is also contaminated by the N V absorption, so that only the blue wing can be fitted. In consequence, both the radial velocity correction and the wavelength calibration that was discussed in Sect. 2 are important for deriving H I column densities.

Table 2. H I column densities towards our Cyg OB2 sample. Errors in log(N(H I)) are $\pm$0.05 or better, except for Cyg OB2#7 and #10, for which we estimate $\pm$ 0.1. E(B-V) values from Massey & Thompson (1991)

Ident	Spectral Type	E(B-V)	log N(H I)
7	O3 If	1.76	21.60
11	O5 If$^+$	1.60	21.85
8C	O5 If	1.54	21.75
8A	O5.5 I(f)	1.79	21.80
4	O7 III((f))	1.50	21.77
10	O9.5 I	1.86	21.95
2	B1 I	1.37	21.80

We follow the usual method (see, e.g., Jenkins, 1970 and Bohlin, 1975), where the L$_\alpha$ profile is assumed to be a pure damping profile, $\sigma(\lambda)$ (see also Shull & Van Steenberg, 1985), so that the rectified flux at λ is given by exp($-\sigma(\lambda)$N(H I)), N(H I) being the neutral hydrogen column density in the direction of the object.

Results are given in Table 2, and obviously the H I column densities towards Cyg OB2 are quite large, with logarithms in the range 21.6–22.0 (compare for example with Fig. 2 of Shull & Van Steenberg, displaying H I column densities towards 244 stars observed with IUE). Errors in our N(H I) values are estimated to be $\pm$0.05 dex, except for Cyg OB2#7 (for which we could not exactly determine the point at which L$_\alpha$ begins to desaturate) and Cyg OB2#10, for which fits at log(N(H I)) equal to 21.95 and 22.00 could not be distinguished.

In Table 2 we also give the E(B-V) values taken from Massey & Thompson (1991). We derive an average value of $< \frac{\log N(\mathrm{HI})}{E(B-V)} >= 21.59 \pm 0.10$. This is somewhat lower than the value given by Shull & Van Steenberg (21.63) for disk stars at the distance of Cyg OB2. Our numbers indicate not only a rather large H I column density towards Cyg OB2, but they also indicate a slightly different compostion of interstellar medium close to Cyg OB2, maybe with some dust still left causing the extra reddening, as suggested in the recent work by Kn¨odlseder (2000).

5. Analysis of the resonance lines

We use the method described by Haser (1995, see also Lamers et al., 1999) to analyse the UV P Cygni lines in order to derive wind terminal velocities, wind column densities of the metal ions, ionization fractions and velocity dispersions.

The first step is to correct for the underlying photospheric components, which we do in an approximate way, by using IUE spectra of hot stars with weak winds (and projected rotational velocities as low as possible) as templates. These tem-

plates have been convolved with appropriate rotational profiles, to account for the individual stellar rotational speeds.

For all stars up to spectral type O7, the spectral regions around N V and C IV have been taken from the hot suddwarf BD+75 325, while for the Si IV profile 15 Mon (O7V) and 9 Sgr (O4V) where chosen for Cyg OB2#4 and for all hotter objects, respectively. For Cyg OB2#10, we have used 10 Lac (O9.5V) as a template for all photospheric profiles.

For Cyg OB2#2 (B1I) we applied a special procedure, with C IV the only profile which has been analyzed here. The underlying photospheric profile had to be created in a somewhat artificial way, because C IV shows a P-Cygni profile with strong blue absorption even at B1V, so that we could not find any appropriate template. To overcome this problem, we simply assume that the photospheric components of C IV behave as those from Si IV except for the different doublet separation, and created an artifical photospheric C IV profile from the purely photospheric Si IV line HD 39 777 (B1.5V).

When deriving wind terminal velocities, it is important to account for the velocity dispersion $v_{\rm turb}$ (usually termed as "turbulent velocity") present in those winds, to correctly reproduce the position of the emission peak, the blue through and the slope of the blue absorption, as originally proposed by Hamann (1981, see also Groenewegen & Lamers, 1989 and Puls et al., 1993, for a further discussion). However, as has been shown by Haser (1995), $v_{\rm turb}$ has to be an increasing function of stellar radius to simultaneously fit all these three features and to be (also physically) consistent with the observational fact that the velocity dispersion in the sub/transonic region (the famous "micro-turbulence") is at most of order sound-speed. Thus we adopt, following Haser (1995), a parameterization of the form

$$v_{\rm turb} = a_t v(r) + b_t, \qquad (1)$$

i.e., the turbulent velocity is assumed to be (roughly) proportional to the local wind-speed $v(r)$, and the coefficients are defined by

$$a_t = \frac{v_{ta} - v_{ti}}{1 - v_{\rm min}}; \qquad b_t = v_{ta} - a_t,$$

where $v_{ti} = v_{\rm turb}(v = v_{\rm min})$ is the minimum turbulent velocity (chosen to be of order sound-speed) and $v_{ta} = v_{\rm turb}(v = v_\infty)$ the maximum one. Note that the latter value is one of the actual fit parameters of the problem.

The velocity stratification is parameterized as a usual β-law,

$$w(x) = (1 - b/x)^\beta \qquad (2)$$

with

$$w(x) = \frac{v(x)}{v_\infty}, \qquad x = r/R_*, \qquad b = (1 - w_{\rm min}^{1/\beta})$$

and $w_{\rm min}$ the ratio of the velocity at x=1 to the terminal velocity, fixed at a value of 0.01.

Table 3 gives the adopted stellar parameters, while the fit results with respect to the wind and turbulent velocity (v_∞, β, v_{ta}) and are listed in Table 4. The final fit to each line is shown in Figs. 3 and 4.

Column densities for metal ions have been derived using the expression given by Haser (1995, see also Howarth & Prinja, 1989 and Lamers et al.,1999):

$$N^{col}(w_1, w_2) = \frac{m_e c}{\pi e^2} \frac{v_\infty}{f_{lu}\lambda_{lu}} \frac{1}{\beta b} \int_{w_1}^{w_2} k(w) w^{1/\beta - 2} dw \qquad (3)$$

where $N^{col}(w_1, w_2)$ is the column density of the ion under consideration, between velocities (in units of v_∞) w_1 and w_2. f_{lu} and λ_{lu} are the oscillator strength and the wavelength of the transition considered, and $k(w)$ is the line strength derived from the fit in parallel with the other fit quantities representing the velocity law. (The latter has to be unique for all lines of a specific star, of course).

All other symbols have their usual meanings. Values for N^{col} are listed in Table 4.

Having derived the column densities for each ion, one can further calculate the product of mean (with respect to w_1, w_2) ionization fraction and mass-loss rate $\dot{M}$ (same references as above):

$$\overline{X_k}\dot{M} = \frac{4\pi m_{\rm H}(1 + 4Y_{\rm He})}{A_k} \beta b R_* v_\infty N^{col}(w_1, w_2) I(w_1, w_2) \qquad (4)$$

with

$$I(w_1, w_2) = \left(\int_{w_1}^{w_2} w^{1/\beta - 2} dw\right)^{-1}. \qquad (5)$$

$A_k = \frac{N({\rm Ion_k})}{N({\rm H})}$ is the element abundance by number and $Y_{\rm He}$ the corresponding He abundance. The latter has been derived from the analysis of photospheric spectra. For the abundances of C, N and Si we followed Lamers et al. (1999) by adopting their "solar" values, i.e., $A_{\rm C} = 3.31 \cdot 10^{-4}$, $A_{\rm N} = 6.92 \cdot 10^{-5}$ and $A_{\rm Si} = 3.98 \cdot 10^{-5}$ for all stars with $Y_{\rm He} \leq 0.1$ (corresponding to $\epsilon \leq 0.09$ in Table 3). For Cyg OB2#7 and #2, we used the abundances they have suggested for O supergiants. Results for $\overline{X_k}\dot{M}$ are listed in Table 5.

6. Individual comments

We briefly comment here on individual aspects of the analysis that could be of interest.

6.1. Cyg OB2#7

Stellar parameters have been taken from the spherical hydrodynamical analysis by Herrero et al. (1999), opposite to all other parameters in Table 3 which come from hydrostatic plane-parallel models.

6.2. Cyg OB2#11

No particular comments.

Table 3. Stellar parameters adopted for the observed stars, with $\epsilon = \frac{N(\mathrm{He})}{N(\mathrm{H})+N(\mathrm{He})}$. References are: (1) Herrero et al. 2000; (2) Herrero et al. 1999; (3) this work.

Ident	Spectral Type	$T_{\rm eff}$	$\log g$	ϵ	$V_{\rm r} \sin i$	$R/R_\odot$	$\log(L/L_\odot)$	Ref.
7	O3 If	50.0	3.72	0.18	105	16.7	6.20	1
11	O5 If$^+$	43.0	3.42	0.09	120	22.4	6.17	2
8C	O5 If	48.0	3.77	0.09	145	13.3	5.93	2
8A	O5.5 I(f)	44.0	3.51	0.09	95	28.4	6.44	3
4	O7 III((f))	39.0	3.52	0.07	125	13.9	5.60	2
10	O9.5 I	31.0	3.11	0.09	85	31.6	5.92	2
2	B1 I	26.0	3.10	0.15	50	14.4	5.06	3

6.3. Cyg OB2#8C

Two different values for the wind column density of C IV are given, because the line fit offers two possibilities, depending on the way the line strength behaves in the inner part of the wind. The maximum value corresponds to a fast increase of line strength inwards, while the minimum corresponds to a smoother increase. The larger value results from a somewhat better fit and is preferred, but the lower one is also possible.

6.4. Cyg OB2#8A

This object has not been analyzed previously in the optical. Its spectrum is quite similar to Cyg OB2#8C, although the He I lines, the H_γ wings and the Of features are slightly weaker than in the latter. All this agrees with the relative spectral classifications. The photometry by Massey & Thompson (1991) gives a very bright visual magnitude (it is the brightest object in their list of blue Cyg OB stars), which results in a high luminosity (the highest one in Table 3), which also results in a very large mass-loss rate ($27.05 \cdot 10^{-6} \mathrm{M}_\odot/\mathrm{yr}$), when the present Galactic WLR is used. This large mass-loss rate however agrees well with the one derived from radio measurements ($29 \cdot 10^{-6} \mathrm{M}_\odot/\mathrm{yr}$, see Leitherer et al., 1982). Of course, a consistent analysis of the optical spectra by means of spherical models is required here (to be given in our follow-up paper), but the present uncertainties do not affect the major results of this paper.

Cyg OB2#8A is the only star for which Leitherer et al. (1982) were able to derive terminal velocities from IUE spectra. Their value of v_∞= 3200 km s^{-1}is much larger than our result of v_∞= 2650 km s^{-1}, related to their neglect of the influence of $v_{\rm turb}$.

All other objects in common with the sample of Leitherer (where the terminal velocities had been derived indirectly from observations of different stars with similar spectral type, cf. Sect. 1) suffer from the same problem, so that their values are systematically larger than ours.

6.5. Cyg OB2#4

See comments for Cyg OB2#8C.

6.6. Cyg OB2#10

The fit to the UV profiles gives comparable results for a combination of v_∞= 1600 km s^{-1}, $v_{\rm turb}$= 350 km s^{-1} and a combination of v_∞= 1700 km s^{-1}, $v_{\rm turb}$= 250 km s^{-1}. We adopt the intermediate value, v_∞= 1650 km s^{-1}, $v_{\rm turb}$= 300 km s^{-1}, and enlarge the typical uncertainties by 50%.

6.7. Cyg OB2#2

The optical spectrum of this star is similar to that of HD 227 634 (B0 Ib), except for the larger projected rotational speed of the latter (Herrero et al., 1992) and slightly weaker He II in the former. The final stellar parameters resulting from a plane-parallel analysis are given in Table 3. These parameters are not completely compatible with a B1 supergiant, however also the rather weak Si IV and C IV features indicate a lower luminosity class, either at B0 or B1.

In Fig. 6.7 we compare the Si IV and C IV profiles of Cyg OB2#2 with those of HD 24 398 (B1 Ib) and HD 147 165 (B1 III), which suggests that Cyg OB2#2 could be of type B1 II and which is also consistent with the observed strong H_α absorption.

Such a lower luminosity class has also other consequences. The individual distance obtained by Massey & Thompson for this star (3.8 kpc) is much larger than the canonical distance to Cyg OB2 (1.7 kpc), which is partly due to its adopted $M_{\rm v}$= -6.4 (corresponding to a Iab luminosity class).

If we, the other way round, assume also for this star the distance to Cyg OB2, this would result in a low absolute magnitude for this star (-4.6), which is much more compatible to the optical, H_α and the UV spectrum, however, of course, forbids a classification as a supergiant.

Adopting finally a luminosity class II as indicated by the UV (see above), this would still result in a rather low absolute magnitude (-4.9) at the distance of Cyg OB2, but now much closer to the typical value for this stellar class (-5.4).

This dilemma and the corresponding uncertainties are not important for the results presented in this paper, but has to be clarified before this star could be used as a data point in the WLR of Cyg OB2.

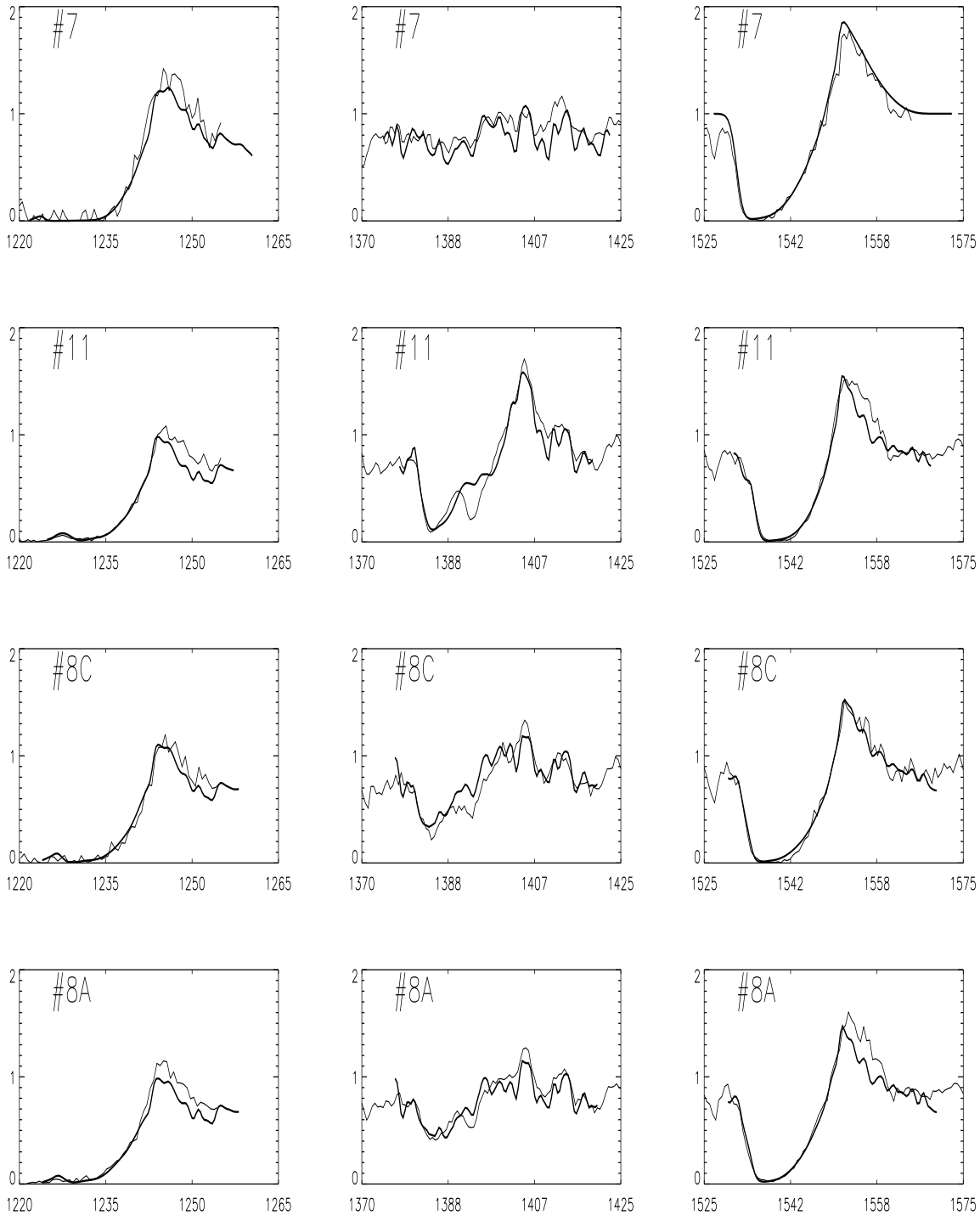

Fig. 3. Final fits for the four hotter stars of our sample. Lines are plotted from left to right (N V, Si IV, C IV) and stars from top to bottom in the same order as they are listed in the tables.

7. Results and Discussion

Table 4 lists terminal velocities, β exponents, values for the fitted turbulence velocity in the outer wind, v_{ta} and metal ion column densities obtained for all stars. In the following, we will present and discuss these and derived results in some detail, where necessary.

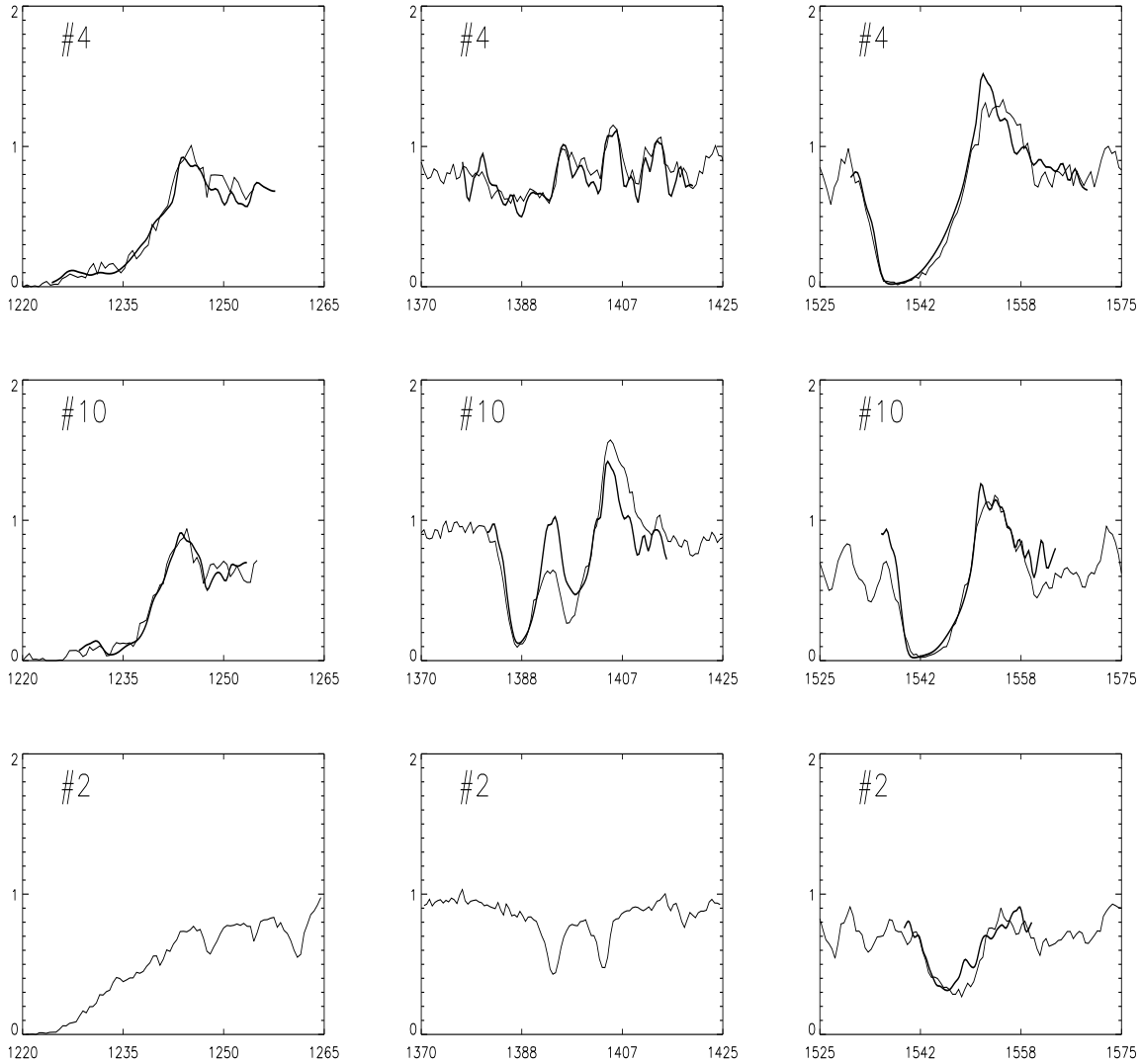

Fig. 4. As Fig. 3, however for the three cooler stars. in the sample. For Cyg OB2#2, only C IV has been fitted.

Turbulence velocities. For all our objects, the ratio v_{ta}/v_∞ is of order 10 to 14%, except for star #10, where we find a rather large value of 18%. These values are in good agreement with the compilation by Haser (1995), who found comparable values for Galactic supergiants, as well as similar high values for a number of supergiants around spectral type O9.

Velocity law. The steepness of the velocity law derived by our UV analysis ($\beta = 0.7 \ldots 0.8$) agrees well with results of comparable investigations (e.g., Groenewegen & Lamers, 1989, Haser, 1995). For star #7, the only star of the present sample which we have already analyzed in the optical by means of spherical models (Herrero et al., 2000), our present value from the UV (0.8) actually coincides with the value found in the latter investigation, where the primary indicator was H_α.

We also like to point out, however, that the results of our present sample (although small) do not show any trend indicated by the investigation by Puls et al. (1996), namely that supergiants typically have a somewhat flatter velocity law, with $\beta \approx 1$. Note, however, that this indication bases on values derived again from H_α which are more sensible in recording the density- (and thus velocity-) stratification of the wind, due to the ρ^2 dependency of line opacity in recombination lines. Nevertheless, in view of the large data bases for derived β-values both from UV and from H_α (and although there are cases where the UV and the H_α value agree, see above), there seems to be a certain trend that, on the average, UV analyses yield lower values for β than H_α. Further and more detailed investigations are necessary to solve this problem (clumping?).

Terminal velocities of our sample agree well with the average v_∞ vs. spectral class relation provided by Kudritzki & Puls (2000), except for Cyg OB2#8A and 8C, which are 25% above

Table 4. Results obtained for the observed stars. v_∞ and v_{ta} (turbulence velocity in outer wind) are given in km s^{-1}, and N(X) is the column density of ion X given in ions cm^{-2}, between w = 0.2 and 1.0. Errors in v_∞ and v_{ta} are 50 km s^{-1}, except for Cyg OB2#10, for which we adopt 75 km s^{-1}. The sum of both velocities is better determined and has also an error of 50 km s^{-1}. Errors in β are $^{+0.15}_{-0.10}$ in all cases. Errors in metal ion column densities are ±0.3 dex for values derived from (partially) saturated lines (mostly N V, C IV) and ±0.1 dex for values from unsaturated lines (mostly Si IV)

Ident	Spectral Type	v_∞	v_{ta}	β	log N(N V)	log N(Si IV)	log N(C IV)
7	O3 If	3080	350	0.7	17.67	14.32	16.51
11	O5 If$^+$	2300	350	0.8	16.17	15.45	16.58
8C	O5 If	2650	300	0.8	16.96	14.96	16.74–17.52
8A	O5.5 I(f)	2650	310	0.7	16.33	14.77	16.26
4	O7 III((f))	2550	350	0.7	15.92	14.64	16.69–17.55
10	O9.5 I	1650	300	0.8	15.70	15.31	16.31
2	B1 I	1250	120	0.8	—	—	15.12

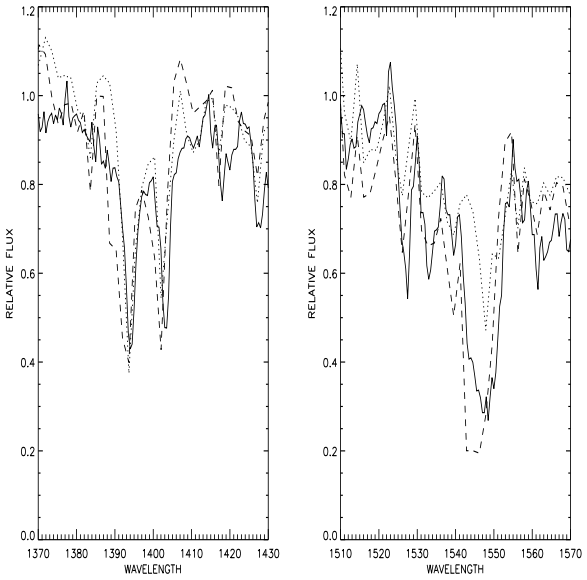

Fig. 5. A comparison of Si IV (left) and C IV (right) line profiles in Cyg OB2#2 (solid), HD 24 398 (B1 Ib, dashed) and HD 147 165 (B1 III, dotted).

the average relation. This is however still within the normal scatter of the relation.

The discussion of the ratio of wind terminal to escape velocity is affected by the well-known problem of the mass discrepancy, i.e., the fact that masses derived from spectroscopic analyses are systematically lower than those obtained from evolutionary models without rotation. The theory of radiatively driven winds predicts for the O-star domain (i.e., if the force-multiplier parameter δ is small, cf. Friend & Abbott 1986; Kudritzki et al. 1989)

$$v_\infty \simeq 2.24 \frac{\alpha}{1-\alpha} v_{\rm esc},$$

with $v_{\rm esc}$ the escape velocity and α one of the line force multiplier parameters (roughly the coefficient in the exponent of the line strength distribution function). The more general relation provided by Kudritzki & Puls (2000, Eq. 15) accounting for additional corrections which are necessary in cases where, e.g., δ is large, leads to essentially the same results in the spectral region discussed here.

Inserting typical values for OB stars, α= 0.6–0.7, we obtain values of 3.3–5.2 for the ratio of terminal to escape velocity.

Fig. 6 displays the correlation between escape and terminal velocity, using both the spectroscopic and the evolutionary masses derived for our objects. Although the diagram based on evolutionary masses shows a good linear correlation between both quantities, the diagram based on our spectroscopic masses is in better agreement with the theoretical predictions, as indicated by a comparison with lines of slope 3.3 and 5.2 (see above). This result is in complete agreement with the findings by Herrero et al. (2000), and we refer the reader to that paper for further discussion.

Column densities and product $\overline{X}\dot{M}$. In Table 4 we have listed the column densities of N V, Si IV and C IV between w =0.2 and w =1.0. Individual errors are ±0.3 for values derived from (partially) saturated lines (mostly N V, C IV) and ±0.1 for values from unsaturated lines (mostly Si IV). For Cyg OB2#8C and Cyg OB2#4 two values are given for C IV because two fits were possible (see previous section for comments).

Using these column densities, the stellar and wind parameters adopted and derived in this work and Eq. 4, we can calculate the product of mean ionization fraction times mass-loss rate. This quantity is tabulated in Table 5, where we show not only the result for an averaging range between w = 0.2 and 1.0, but also for the range w= 0.4 and 1.0. A comparison of both values gives us an idea about how representative these mean ionization fractions are for the conditions in the whole wind and especially how sensible they are if the lower wind (where the fitted run of opacity becomes questionable) does no longer contribute to the mean value.

Fortunately, the variations are small (always below 0.2 dex), except in the two cases of C IV where we preferred the possibility of an extremely steep increase of $k(w)$ inwards (Cyg OB2#8C and #4, cf Sect. 6). Since here the number of absorbing atoms increases rapidly inwards, the mean ionization frac-

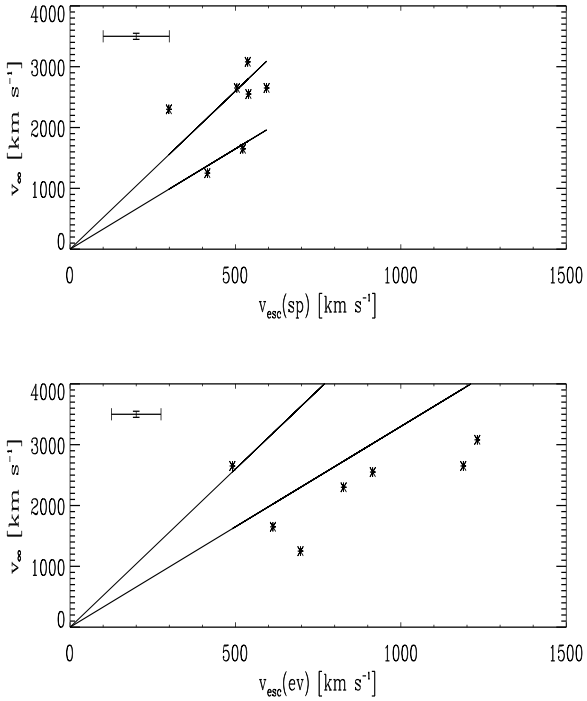

Fig. 6. Wind terminal velocities of Cyg OB2 stars as function of their escape velocities, obtained from spectroscopic (above) and evolutionary (below) masses. The lines have slopes predicted by theory for α values of 0.6 and 0.7, e.g., 3.3 and 5.2. Typical error bars have been plotted in the upper right corner.

tion becomes considerably larger ($\approx$ 0.6 dex) when the more extended averaging range is considered.

Individual errors are dominated by errors in the column densities, and are $\pm$0.33 and 0.14 for $\overline{X}\dot{M}$ for the ions N V and Si IV respectively, and $\pm$0.3... 0.4 for C IV, depending on the adopted C abundance (the larger value corresponds to objects with large Helium abundance, for which the C abundance quoted by Lamers et al., 1999, has a larger error).

Mean ionization fractions using the present Galactic WLR. Although we have not yet analyzed the mass-loss rates of our sample stars (except for star #7), we like to give an impression of one the most interesting quantities resulting from our investigation, namely the mean ionization fraction itself. To this end, we will use the present Galactic WLR as defined by Puls et al. (1996) (see also Kudritzki & Puls, 2000) to calculate mass-loss rates which should be not too erroneous since almost all of our stars are supergiants and since the distance to Cyg OB2 is well defined. If all mass-loss rates will have been derived finally, it will be easy to specify the mean fractions in a more precise way. However, we do not expect *dramatic* differences.

From the WLR and the luminosities, terminal velocities and stellar radii derived in this work we obtain mass-loss rates as outlined in Table 6. Comparing at least to the actual H_α mass-loss rate of $\dot{M}$ = 11.22 $\cdot 10^{-6} M_\odot/\mathrm{yr}$ known for star #7 (Herrero et al., 2000), the agreement is satisfactory.

Table 7. Average values for mean ionization fractions obtained from different authors and different samples. Errors relate only to the standard deviation from the mean, see text. (1): Howarth & Prinja, 1989; (2): Lamers et al., 1999; (3): present work

Ref.	$\overline{X}$(N V)	$\overline{X}$(Si IV)	$\overline{X}$(C IV)
1	-2.57±0.61	-3.56±1.07	-2.86±0.44
2	-2.65±0.69	-2.93±0.45	-2.53±0.54
3	-2.45±0.45	-3.63±0.45	-2.70±0.73

Again for both averaging ranges, w = [0.2,1.0] and w = [0.4,1.0], the resulting mean ionization fractions are given in Table 6. Of course, the relative behaviour of the two zones is the same as before. The individual errors, however, are now very large, because they are dominated by the uncertainty in the mass loss rate, as a direct consequence of the relatively large scatter in the present Galactic WLR (cf. Sect. 1).

We estimate the uncertainty in our ionization fractions to be at least $\pm$0.8 in log($\overline{X}_k$), which will be improved when our project of deriving individual mass-loss rates has succeeded.

It is interesting to compare our values with those from other authors. For the resonance lines analyzed here, our definition of mean ionization fraction coincides with the $< q >$ values defined by Lamers et al. (1999), as well as with the definition introduced by Howarth & Prinja (1989). Thus we can compare directly our results with those by them.

At first, let us concentrate on the straight average of mean ionization fractions, using all values in the respective samples. With respect to N V, Si IV and C IV this is done in Table 7. Within the "error" bars, all investigations agree with each other. Note that for our comparison we have tabulated only the standard deviation from the mean, excluding any additional, individual errors which can be quite large.

Nevertheless, there is a trend for our values to be in better agreement with those by Howarth & Prinja than with those by Lamers et al., in particular for Si IV. We have to admit, however, that our sample is comparable to the others only to a limited extent, because (a) our sample is much smaller, (b) we have investigated almost only supergiants and (c) the mass-loss rates are only correct within the scatter of the present WLR. Anyway, we consider the results sufficient to conclude that we do not see any substantial differences.

In a final step, we like to illuminate the primary dependencies of the mean ionization fractions for our sample, in the same spirit as performed by Lamers et al. In accordance with these authors, we expect a dependence on $T_{\rm eff}$ and mean density $< \rho >$. The latter quantity is the density at that point where half the terminal velocity is reached in the wind ($r_{0.5}$). Since our sample consists almost only of supergiants (in contrast to the one by Lamers et al.), we have, following again these authors, to check whether there is now a correlation between those two parameters, where such a correlation has not been found by Lamers et al. in their sample.

Table 5. Product of mean ionization fraction times mass-loss rate for Cyg OB2 stars; averaging range w = [0.2,1.0] (left) and w= [0.4,1.0] (right), see text.

Ident	Spectral Type	log $\overline{X}$(N V)$\dot{M}$	log $\overline{X}$(Si IV)$\dot{M}$	log $\overline{X}$(C IV)$\dot{M}$	log $\overline{X}$(N V)$\dot{M}$	log $\overline{X}$(Si IV)$\dot{M}$	log $\overline{X}$(C IV)$\dot{M}$
7	O3 If	-0.81	-3.15	-1.88	-0.70	-3.15	-1.61
11	O5 If$^+$	-1.66	-2.14	-1.94	-1.58	-2.02	-1.94
8C	O5 If	-1.04	-2.80	-1.94 – -1.17	-1.21	-2.68	-2.09 – -1.80
8A	O5.5 I(f)	-1.34	-2.66	-2.10	-1.34	-2.58	-2.09
4	O7 III((f))	-2.12	-3.15	-2.02 – -1.16	-2.12	-3.15	-2.18 – -1.78
10	O9.5 I	-2.14	-2.28	-2.21	-1.98	-2.16	-2.18
2	B1 I	—	—	-3.38	—	—	-3.38

Table 6. Mass-loss rates (in units of 10^{-6} $M_\odot$/year) and mean ionization fractions for the Cyg OB2 stars, assuming the present Galactic WLR for O-supergiants. Averaging ranges as in Table 5.

Ident	Spectral Type	$\dot{M}$	log $\overline{X}$(N V)	log $\overline{X}$(Si IV)	log $\overline{X}$(C IV)	log $\overline{X}$(N V)	log $\overline{X}$(Si IV)	log $\overline{X}$(C IV)
7	O3 If	12.89	-1.92	-4.26	-2.72	-1.81	-4.26	-2.72
11	O5 If$^+$	13.39	-2.79	-3.27	-3.07	-2.70	-3.15	-3.07
8C	O5 If	6.40	-1.85	-3.61	-2.75 – -1.97	-2.01	-3.48	-2.90 – -2.60
8A	O5.5 I(f)	27.05	-2.77	-4.09	-3.53	-2.77	-4.01	-3.52
4	O7 III((f))	2.00	-2.42	-3.46	-2.33 – -1.46	-2.42	-3.46	-2.48 – -2.08
10	O9.5 I	6.44	-2.94	-3.09	-3.01	-2.79	-2.97	-2.98
2	B1 I	0.58	—	—	-3.14	—	—	-3.14

In contradiction to their findings, however, we see from Fig. 7 that $T_{\rm eff}$ and $<\rho>$ are tightly correlated. To understand this difference, let us proceed as follows. Using the definition of $<\rho>$,

$$<\rho>=\frac{\dot{M}}{4\pi r_{0.5}^2}\frac{2}{v_\infty}\propto\frac{\dot{M}}{R_*^2 v_\infty}f(\beta),\ f(\beta)\approx 1-0.5^{\frac{1}{\beta}} \qquad (6)$$

and the WLR (assuming $\alpha'=\alpha-\delta$ to be close to a value of 2/3)

$$\log(\dot{M}v_\infty R_*^{0.5})\approx\frac{1}{\alpha'}\log(L)+D(k,\alpha') \qquad (7)$$

with k,α,δ the line force multiplier parameters and $D(k,\alpha')$ the vertical offset, different for different ranges in spectral type, luminosity class, metallicity and He-content (cf. Puls et al.,1996 and Kudritzki & Puls, 2000), we easily obtain

$$\log<\rho> \approx \frac{4}{\alpha'}\log(T_{\rm eff})+(\frac{2}{\alpha'}-\frac{5}{2})\log(R_*)+ + \log\frac{f(\beta)D(k,\alpha')}{v_\infty^2}+\text{const.} \qquad (8)$$

In order to avoid any consideration of stellar masses, mass–luminosity relation and Eddington factors Γ if a relation $v_\infty^2\propto v_{\rm esc}^2\propto M/L(1-\Gamma)$ would be used (an alternative way that leads to a similar result as the one we present here), we simplify this equation by means of an average $v_\infty\propto T_{\rm eff}$ relation, as derived for example from Table 1 or Fig. 4 of Kudritzki & Puls (2000) (although this relation results in a significant scatter).

$$\log<\rho> \approx (\frac{4}{\alpha'}-2)\log(T_{\rm eff})+(\frac{2}{\alpha'}-\frac{5}{2})\log(R_*)+ + \log\big(f(\beta)D(k,\alpha')\big)+\text{const}'. \qquad (9)$$

This equation clearly explains why in our case of considering O-type supergiants with similar values of β and $\alpha'\approx 2/3$, i.e.,

$$\log<\rho>\approx 4\log(T_{\rm eff})+\frac{1}{2}\log(R_*)+\text{const}'', \qquad (10)$$

the mean density is such strongly correlated with $T_{\rm eff}$ and that the extra dependency on stellar radius should be very weak.

In fact, by performing a multi-linear regression of $\log<\rho>$ with respect to $\log T_{\rm eff}$ and $\log R_*$, we obtained a temperature coefficient of 3.24 and a radius coefficient of 0.41, close to the approximation of Eq. 10.

This primary dependence of mean wind density on effective temperature, if one considers a single luminosity class in a well defined spectral range, can be actually also found in Fig. 2 of Lamers et al. (1999), where we see that different luminosity classes give actually good correlations of $<\rho>$ versus $T_{\rm eff}$, if one allows for a shift in vertical offset. At a given $T_{\rm eff}$, a change in luminosity class means a change in the wind dynamics, that reflects in a change in the wind parameters β, κ, α and δ, and in a change in $<\rho>$.

Thus it is not surprising at all that we find the same dependence of mean ionization fractions on both $T_{\rm eff}$ and $<\rho>$, as can seen in Fig. 8. In so far, we will compare here only the dependence on $T_{\rm eff}$ with the according analysis by Lamers et al. (their Figs. 3a,c,e), whereas a comparison with the behaviour as function of mean density is prohibitive due to the missing luminosity classes II to V. (Note also that to explain the behaviour of the ionization fractions with $<\rho>$ we need to simultaneously consider the changes in the wind parameters). To make it short, our analysis of the ionization fractions of O-*supergiants* results in the same correlations: The mean ionization of N V

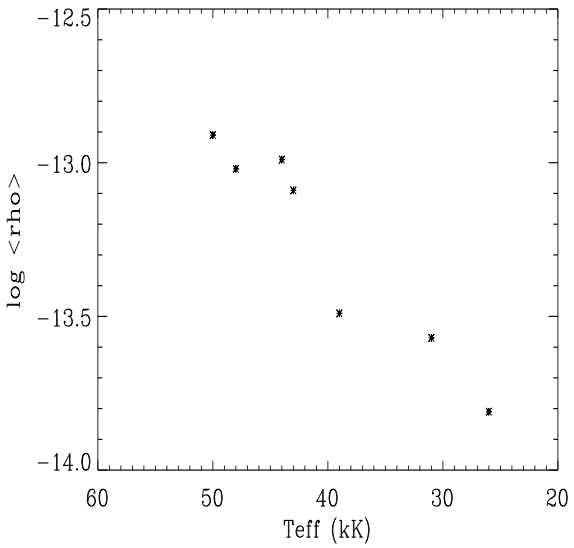

Fig. 7. Mean wind density versus effective temperature for our sample. Compare with Fig. 2 of Lamers et al. (1999). See text for discussion.

increases with $T_{\rm eff}$, Si IV decreases with $T_{\rm eff}$ and C IV seems to be uncorrelated, which simply reflects the change in ionization equilibrium due to an increasing temperature, if there is no extra dependency on density. For further discussion, we refer the reader to Lamers et al.

8. Conclusions and future work

We have observed and analyzed a sample of six O supergiants and one giant that belong to Cyg OB2. In particular we have presented 3 O5 supergiants, a group that is underrepresented in the IUE archive. All spectra show the expected morphology.

Interstellar H I column densities towards Cyg OB2 have been determined from the IS L_α line, which is so strong that it seriously affects the rectification of the continuum close to the stellar N V resonance line. The H I column densities derived are very large, but $< \frac{\log N({\rm HI})}{E(B-V)} >$ is slightly lower than the corresponding value of Shull & Van Steenberg (1985), indicating some extra reddening. This result agrees with Cyg OB2 being a very young association, may be with some dust still left, as suggested by other works (see Massey & Thompson, 1991; Knödelseder, 2000).

We derived terminal wind velocities, turbulent velocities, β values for the velocity law, metal ion column densities and products of mean ionization fractions times mass loss rates, applying standard methods (Haser, 1995; Lamers et al., 1999) to the resonance lines of N V, C IV and Si IV. By using then the present average WLR for the Milky Way we can obtain mean ionization fractions in the wind.

The main objective of this work was to determine wind terminal velocities, which were obtained with a high accuracy. The values found, in the range from 1250 to 3080 km s^{-1}, agree well with the average v_∞ vs. spectral class relationship compiled by Kudritzki & Puls (2000 and references therein). Turbulent velocities are in the expected range from 10 to 14% of the terminal velocity (with one exception).

It is interesting to note that we find β values in the range 0.7 – 0.8. We do not see the trend indicated by Puls et al. (1996) in the sense that O supergiants have somewhat flatter velocity laws with $\beta \approx 1$. As the Puls et al. values are based on H_α data, this points to a difference in the β values derived from H_α and UV (latter being lower).

The observations confirm the existence of the v_∞ vs. v_{esc} relationship, as predicted by the theory of radiation driven winds. However, we encounter the same trend as found in Herrero et al. (2000), namely that spectroscopic masses agree well with the coefficients predicted by that relationship, whereas evolutionary masses do not.

The mean ionization fractions of N V, C IV and Si IV determined are consistent with those from other authors (Howarth & Prinja, 1989; Lamers et al., 1999) in spite of the large uncertainties and the differences in the samples (our sample is much smaller and consists almost only of supergiants) and methods (we derive the mass loss rates using the average Galactic WLR relation).

When trying to explain the behaviour of the mean ionization fractions we find that they show similar trends with $T_{\rm eff}$ and $< \rho >$, the mean density at the point where half the terminal velocity is reached in the wind. We have shown that this is due to the tight relation of $T_{\rm eff}$ and $< \rho >$ for a fixed luminosity class. This result appears to differ from that of Lamers et al. (1999) who state that these two quantities do not correlate. However, inspection of their Fig. 2 indicates actually good correlations for *individual* luminosity classes.

We have determined stellar parameters for Cyg OB2#8A and #2 based on plane–parallel, hydrostatic models, as we have done already before for all other observed objects. The immediate next step will be to consistently derive individual mass loss rates by means of spherical models with mass loss (Santolaya–Rey et al., 1997). At the same time, we continue in our group with the work aimed at calibrating the WLR in different metallicity environments like the Magellanic Clouds, M31 and M33 (see Kudritzki & Puls, 2000, and references therein), which is needed to apply the WLR beyond the Local Group.

Acknowledgements. AH wants to acknowledge support for this work by the spanish DGES under project PB97-1438-C02-01 and from the Gobierno Autonómico de Canarias under project PI1999/008. RPK wishes to thank his colleagues at the Universitätssternwarte München for 18 years of beautiful collaborative work and a wonderful working climate.

References

Bohlin R.C., 1975, ApJ 200, 402
Friend D.B., Abbott D.C., 1986, ApJ 311, 701
Groenewegen M.A.T., Lamers H.J.G.L.M., 1989, A&AS 79, 359
Hamann W.R., 1981, A&A 93, 353
Haser S.M., 1995, PhD Thesis, Universitäts–Sternwarte der Ludwig–Maximillian Universität, München

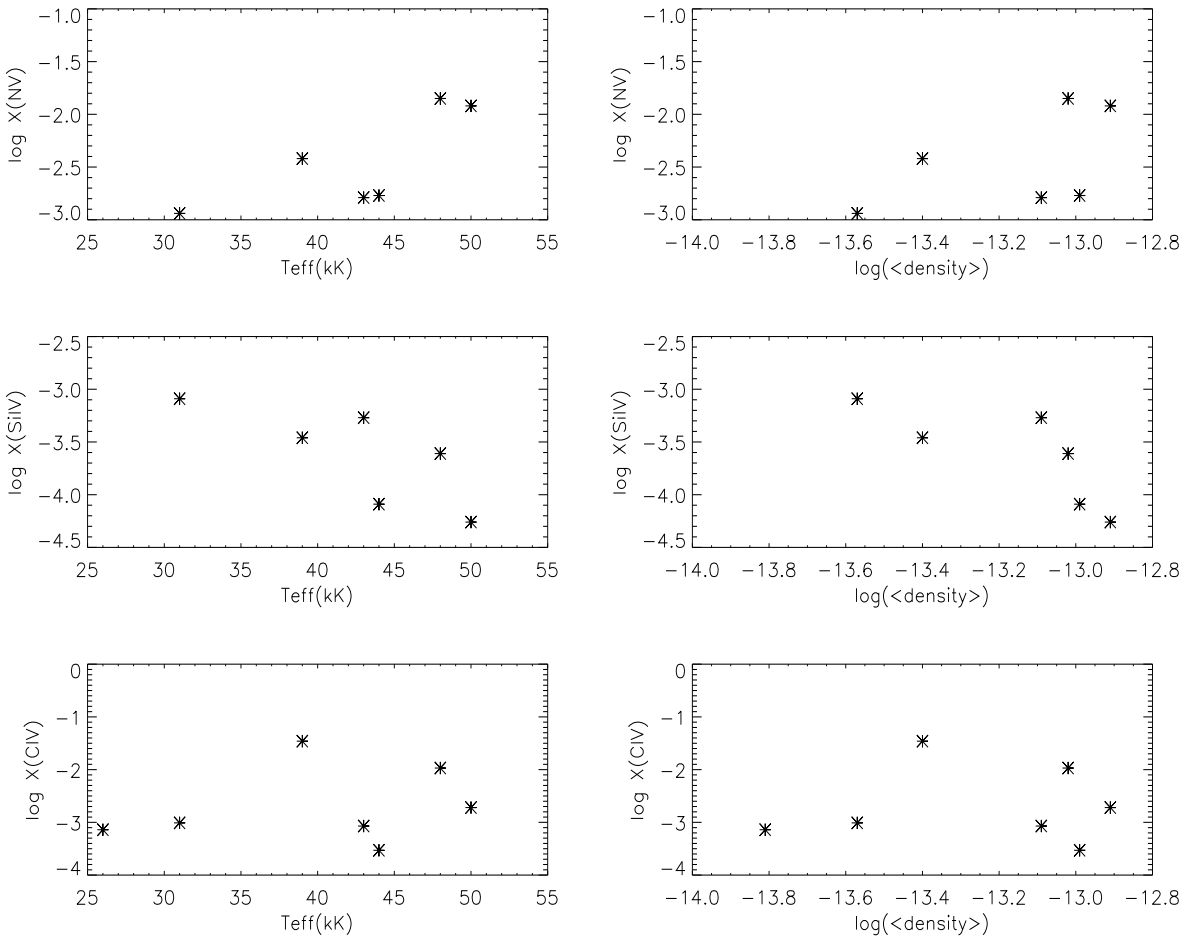

Fig. 8. The mean ionization fractions versus $T_{\rm eff}$ and $< \rho >$. We find a similar behaviour in both cases. See text.

Herrero A., Kudritzki R.P., Vílchez J.M., et al., 1992, A&A 261, 209
Herrero A., Corral L.J., Villamariz M.R., Martín E.L., 1999, A&A 348, 542
Herrero A., Puls J., Villamariz M.R., 2000, A&A 354, 193
Howarth I.D., Prinja R.K., 1989, ApjS 69, 527
Jenkins E.B., 1970, in IAU Symp. 36 on Ultraviolet Stellar Spectra and Ground Based Observations, L. Houziaux & H.E. Butler eds., (Dordrecht: Reidel), p. 281
Knödlseder J., 2000, A&A, in press
Kudritzki R.P., Puls J., 2000, ARA&A in press
Kudritzki R.P., Puls J., Lennon D.J. et al., 1999, A&A 350, 970
Kudritzki R.P., Pauldrach A.W.A., Puls J., Abbott D.C., 1989, A&A 219, 205
Lamers H.J.G.L.M., Haser S., de Koter A., Leitherer C., 1999, ApJ 516, 872
Leitherer C., Hefele H., Stahl O., Wolf B., 1982, A&A 108, 102
Massey P., Thompson A.B., 1991, AJ 101, 1408
McCarthy J.K., Kudritzki R.P., Lennon D.J., et al., 1997, ApJ 482, 757
Puls J., Owocki S.P., Fullerton A.W., 1993, A&A 279, 457
Puls J., Kudritzki R.P., Herrero A., et al., 1996, A&A 305, 171
Santolaya–Rey A.E., Puls J., Herrero A., 1997, A&A 323, 488
Schulte D.H. 1958, ApJ 128, 41
Shull J.M., Van Steenberg M.E., 1985, ApJ 294, 599
Walborn N.R., 1973, AJ 78, 1067
Walborn N.R., Nichols–Bohlin J., Panek R.J., 1985, NASA Ref. Pub. 1155